

# ZACH-ViT: Regime-Dependent Inductive Bias in Compact Vision Transformers for Medical Imaging

Athanasios Angelakis

athanasios.angelakis@unibw.de

ORCID: 0000-0003-1226-9560

<sup>1</sup> BioML Lab, RI CODE, UniBW, Munich, Germany

<sup>2</sup> EDS, Amsterdam UMC, Amsterdam, Netherlands

## Abstract

Vision Transformers rely on positional embeddings and class tokens that encode fixed spatial priors. While effective for natural images, these priors may hinder generalization when spatial layout is weakly informative or inconsistent, a frequent condition in medical imaging and edge-deployed clinical systems. We introduce ZACH-ViT (Zero-token Adaptive Compact Hierarchical Vision Transformer), a compact Vision Transformer that removes both positional embeddings and the [CLS] token, achieving permutation invariance through global average pooling over patch representations. The term “Zero-token” refers specifically to the removal of the dedicated [CLS] aggregation token and positional embeddings; patch tokens are still present and processed normally. Adaptive residual projections preserve training stability in compact configurations while maintaining a strict parameter budget.

Evaluation is performed across seven MedMNIST datasets spanning binary and multi-class tasks under a strict few-shot protocol (50 samples per class, fixed hyperparameters, and five random seeds). The empirical analysis reveals a clear regime-dependent behavior: ZACH-ViT (0.25M parameters, trained from scratch) achieves its strongest advantage on BloodMNIST and remains competitive with TransMIL on PathMNIST, while its relative advantage decreases on datasets with strong anatomical priors (OCTMNIST, OrganAMNIST), consistent with the architectural hypothesis. These results support the view that architectural alignment with data structure can be more important than pursuing universal benchmark dominance. Despite its minimal size and lack of pretraining, ZACH-ViT achieves competitive performance while maintaining sub-second inference times, supporting deployment in resource-constrained clinical environments. Code and models are available at <https://github.com/Bluesman79/ZACH-ViT>.

**Keywords:** Vision Transformers, Few-shot learning, Permutation invariance, Parameter efficiency, Edge AI, Medical imaging, Spatial structure

# 1 Introduction

Vision Transformers (ViTs) have reshaped computer vision through strong performance and scalability on large-scale benchmarks such as ImageNet [1]. Their architecture typically relies on positional embeddings and a [CLS] token, which introduce an implicit bias toward spatially structured representations. While appropriate for natural images, this assumption does not universally hold. In many real-world scenarios, image patches lack intrinsic ordering or spatial relationships carry limited discriminative value.

Several medical imaging modalities illustrate this mismatch. Blood cells appear randomly distributed within microscopy fields; histopathology patches often behave as unordered collections where diagnosis depends on cellular composition rather than spatial arrangement; lung ultrasound frames vary substantially with probe positioning. In such settings, positional priors may introduce unintended bias, encouraging models to exploit spurious spatial correlations instead of invariant visual characteristics.

To address this mismatch between architectural priors and data structure, we introduce ZACH-ViT (Zero-token Adaptive Compact Hierarchical Vision Transformer), a compact architecture designed around permutation-invariant patch processing:

- **Zero-token:** Positional embeddings are removed and the [CLS] aggregation token is replaced with global average pooling, allowing patch tokens to be treated as an unordered set.
- **Adaptive:** Residual projections preserve gradient stability when feature dimensionality changes across transformer layers.
- **Compact:** The architecture operates with 0.25M parameters by avoiding components dedicated to modeling potentially weakly informative spatial structure.
- **Hierarchical:** Multiple transformer layers capture compositional features without introducing positional bias.
- **End-to-end:** Unlike MIL-based transformers designed primarily for bag-level aggregation, ZACH-ViT functions as a standalone compact vision backbone with direct patch-level representation learning.

The resulting model is permutation-invariant by construction while remaining parameter-efficient (0.25M parameters) and computationally lightweight. We evaluate ZACH-ViT across seven representative MedMNIST datasets [2], covering binary classification (BreastMNIST, PneumoniaMNIST) and multi-class tasks (BloodMNIST, DermaMNIST, OCTMNIST, PathMNIST, OrganAMNIST). These datasets span a spectrum of spatial structure strength, ranging from weakly structured blood microscopy images to anatomically constrained abdominal and retinal scans.

Rather than claiming universal superiority, our results reveal a regime-dependent behavior: ZACH-ViT performs strongest when spatial order is weakly informative (BloodMNIST, PathMNIST) and remains competitive when anatomical structure imposes fixed spatial relationships (OCTMNIST, OrganAMNIST). This supports the broader hypothesis that architectural inductive biases should

align with the spatial characteristics of the target data instead of assuming uniform spatial relevance.

This perspective is particularly relevant for edge AI deployment in medical imaging, where inference increasingly occurs on scanners, pathology workstations, and hospital-side systems under strict latency, memory, and connectivity constraints. In such environments, models must balance structural robustness with computational efficiency.

Our contributions can be summarized as follows:

- We introduce ZACH-ViT, a compact permutation-invariant Vision Transformer that removes positional embeddings and token-based aggregation, enabling efficient end-to-end patch processing without reliance on spatial priors.
- We provide a systematic regime-spectrum analysis linking transformer inductive bias to spatial structure strength, demonstrating when permutation invariance becomes advantageous under controlled few-shot medical imaging conditions.
- Through a comprehensive benchmark across fifteen architectures and seven MedMNIST datasets under identical protocols, we show that architectural alignment with data structure can be more influential than absolute model scale or pretraining.

Overall, the main contribution of this work extends beyond the architecture itself: we establish a reproducible evaluation framework for studying when permutation-invariant transformers are appropriate in medical imaging, shifting the focus from absolute benchmark dominance toward principled inductive-bias alignment.

## 2 Related Work

### 2.1 Permutation-Invariant Vision Architectures

A preliminary arXiv preprint introduced the ZACH-ViT architecture on a clinical lung ultrasound dataset [3]. Subsequent analysis revealed annotation issues in that dataset, preventing reliable clinical conclusions. The present work therefore provides a structured and controlled evaluation across seven MedMNIST datasets, enabling a systematic analysis of how permutation-invariant architectures behave under varying spatial-structure regimes.

The present work provides a structured empirical validation of ZACH-ViT across seven MedMNIST datasets spanning weak to strong spatial structure under consistent few-shot protocols. The analysis reveals a clear regime-dependent behavior, consistent with the architectural hypothesis: removing positional priors is not universally beneficial, but becomes advantageous when spatial layout is weakly informative. This broader validation was not possible in the earlier clinical study due to data limitations and narrow task scope.

### 2.2 Distinction from MIL-based Transformers.

TransMIL [4] also operates on unordered sets of patch representations within a multiple-instance learning (MIL) framework, resulting in permutation-invariant

aggregation at the bag level. However, the design objectives differ substantially from ZACH-ViT. TransMIL is primarily developed for whole-slide imaging, where transformers are used as an aggregation mechanism over pre-extracted instances within a MIL pipeline. In contrast, ZACH-ViT is a compact transformer backbone explicitly designed for end-to-end few-shot learning under strict parameter and edge-deployment constraints. The contribution of ZACH-ViT therefore lies not in introducing permutation invariance itself, but in demonstrating how removing positional priors within a minimal transformer architecture interacts with spatial-structure regimes across datasets. This distinction is supported by the regime-spectrum analysis, which reveals when permutation-invariant design is advantageous and when positional structure becomes beneficial. Importantly, TransMIL operates on pre-extracted instance embeddings within a multiple-instance learning (MIL) pipeline and applies transformer layers as a bag-level aggregator. In its original formulation, spatial relationships between instances are modeled through relative positional cues derived from instance coordinates, while the transformer itself is not designed as a compact end-to-end vision backbone. In contrast, ZACH-ViT performs direct patch-level representation learning from images without an MIL preprocessing stage, removes positional encodings entirely, and enforces permutation invariance through global average pooling. Thus, although both methods may process unordered sets, they differ fundamentally in objective, architectural role, and deployment constraints.

### 2.3 Positional Embedding Removal Across Domains

The idea that positional encodings may act as unnecessary or even harmful inductive biases has recently emerged in multiple domains. In language modeling, Gelberg et al. [5] showed that removing rotary positional embeddings after pretraining (DroPE) enables improved context-length extrapolation in large language models. Although developed in a different setting, this observation is conceptually aligned with our work in questioning whether positional information should always be embedded as a permanent architectural prior.

Despite this conceptual overlap, the underlying challenges differ substantially. DroPE addresses sequence extrapolation in language models where positional information is intrinsic but becomes out-of-distribution at longer context lengths. In contrast, ZACH-ViT targets medical imaging scenarios in which spatial information is frequently weakly informative or non-diagnostic by design. Taken together, these directions suggest a broader principle: architectural components encoding spatial or temporal priors should be matched to the structural properties of the data rather than applied universally. Our regime-spectrum analysis (Figure 1) provides empirical evidence for this principle within medical vision tasks, clarifying when permutation-invariant modeling is most effective.

## 3 Method: ZACH-ViT

### 3.1 Architecture Overview

Given an input image  $X \in \mathbb{R}^{H \times W \times C}$ , ZACH-ViT extracts non-overlapping patches and projects them into a latent space:

$$Z_0 = \text{Linear}(\text{Patchify}(X)) \in \mathbb{R}^{N \times d},$$

where  $N$  denotes the number of patches and  $d$  the embedding dimension. Unlike standard ViTs, no positional embeddings are added, preserving invariance to patch permutations. A stack of transformer blocks processes  $Z_0$ , and the final representation is obtained via global average pooling:

$$h = \frac{1}{N} \sum_{i=1}^N Z_L^{(i)}$$

A linear classifier maps  $h$  to output logits. By removing positional encoding and replacing the [CLS] token with global pooling, permutation invariance is achieved by construction while avoiding parameters dedicated to modeling potentially non-informative spatial relationships.

### 3.2 Adaptive Residual Projections

Compact transformer architectures may exhibit unstable optimization when feature dimensionality changes across layers, particularly under strict parameter constraints. ZACH-ViT addresses this issue through adaptive residual projections. Let  $x$  denote the input to a transformer block and  $y$  its transformed output. Residual summation is defined as

$$x \leftarrow \begin{cases} W_{\text{proj}}x + y, & \text{if } \dim(x) \neq \dim(y), \\ x + y, & \text{otherwise,} \end{cases}$$

where  $W_{\text{proj}}$  is a learnable linear projection initialized to zero. This mechanism preserves gradient flow across dimensional transitions while introducing minimal additional parameters, enabling stable training within the 0.25M-parameter regime. In preliminary experiments without adaptive projections, compact variants with changing feature dimensionality showed occasional optimization instability (training divergence or increased variance across seeds), motivating the inclusion of this lightweight projection mechanism.

## 4 Experimental Protocol

### 4.1 Few-Shot Setting

All experiments follow a unified protocol to ensure consistent comparison:

- 50 training samples per class (randomly sampled from the official training split)
- Validation and test splits kept unchanged

- Batch size: 16
- Learning rate:  $1 \times 10^{-4}$  (AdamW optimizer)
- Epochs: 23
- Random seeds: {3, 5, 7, 11, 13} (reported as mean  $\pm$  standard deviation)

This setup intentionally stresses models under data-scarce conditions representative of real-world medical imaging scenarios.

## 4.2 Spatial Structure Spectrum and Dataset Selection

We evaluate seven datasets from the MedMNIST v2 suite [2], selected to span a broad spectrum of spatial structure while maintaining task compatibility:

- **Very weak (1):** BloodMNIST — blood cells appear randomly distributed in microscopy fields.
- **Weak (2):** PathMNIST — histopathology patches behave as unordered diagnostic collections.
- **Moderate (3):** BreastMNIST (variable ultrasound probe position), PneumoniaMNIST (inconsistent X-ray framing).
- **Strong (4–5):** DermaMNIST (lesion-centered but variable), OCTMNIST (fixed retinal layer structure), OrganAMNIST (stable abdominal anatomy).

Three datasets from MedMNIST were excluded for methodological reasons:

- **ChestMNIST:** multi-label classification task, incompatible with the unified binary/multi-class evaluation protocol.
- **RetinaMNIST:** ordinal regression task requiring specialized evaluation metrics.
- **TissueMNIST:** histopathology modality with visual characteristics highly overlapping PathMNIST, adding limited additional structural diversity.

This selection preserves consistent evaluation metrics while covering the intended spatial-structure spectrum.

## 4.3 Model Families and Benchmarking

We evaluate fifteen models spanning four architectural families, covering different parameter scales, initialization regimes, and inductive biases.

Rather than reporting only selected baselines, all trained models are included in the analysis. This enables comparison from ultra-compact scratch-trained architectures (0.09M parameters) to large pretrained Transformers (85.8M parameters).

Table 1 summarizes the evaluated models.

Subset-specific comparisons (e.g., scratch-only analyses to isolate inductive bias or reduced plots for readability) are explicitly indicated and do not reflect selective reporting.

Table 1: Complete list of evaluated models trained under the identical few-shot protocol. Initialization indicates whether ImageNet-pretrained weights were used. Parameter counts are exact. Disk footprint reports saved weight file size measured on BreastMNIST (seed=7, 50-shot, batch size 16, 23 epochs) to approximate deployment-oriented storage cost. Citations correspond to original architecture publications.

Family	Model	Params (M)	Initialization	Weights (MB)
Scratch Models	ABMIL [6]	0.09	Random	1.082
	<b>ZACH-ViT (Ours) [3]</b>	0.25	Random	<b>2.949</b>
	TransMIL [4]	0.26	Random	3.051
	Minimal-ViT [1]	0.62	Random	7.458
	CNN-ABMIL [6, 7]	1.12	Random	103.205
CNN (ImageNet)	MobileNetV2 [8]	2.39	ImageNet	27.959
	EfficientNetB0 [9]	4.17	ImageNet	48.611
	DenseNet121 [10]	7.09	ImageNet	82.666
	InceptionV3 [11]	22.03	ImageNet	253.120
	ResNet50 [7]	23.80	ImageNet	273.133
Transformers (ImageNet)	DeiT-Small [12]	21.67	ImageNet	82.722
	Swin-Tiny [13]	27.52	ImageNet	105.058
	ViT-B/16 [1]	85.80	ImageNet	327.365
Hybrid / Modern Backbones (ImageNet)	MambaOut-Tiny [14]	24.24	ImageNet	92.555
	ConvNeXt-Tiny [15]	27.92	ImageNet	319.985

Disk footprint complements parameter count by measuring serialized model size under a fixed training configuration, reflecting practical storage and distribution cost relevant to edge deployment and reproducibility.

## 4.4 Implementation and Experimental Environment

All experiments were executed in a controlled Linux environment using Python 3.10.12. ZACH-ViT and all ablation studies were implemented in TensorFlow 2.14.0.

Certain baseline architectures whose official or stable implementations are available only in PyTorch were evaluated using their original implementations (PyTorch 2.2.2, timm 1.0.24). These models were executed under identical dataset splits, training protocols, and hardware settings to ensure comparability.

Experiments were run on a workstation equipped with an NVIDIA RTX A5000 GPU (24 GB VRAM), CUDA 12.8, and 128 CPU cores. The software stack included library\_zViT (version 2026001011), MedMNIST 3.0.2, NumPy 1.24.3, Pandas 1.5.3, Matplotlib 3.10.8, and Scikit-learn 1.2.0.

Random seeds were fixed across runs, and all models used identical preprocessing and data splits to maximize reproducibility.

## 4.5 Evaluation Metrics

Primary evaluation metrics depend on dataset type:

- **Binary datasets** (BreastMNIST, PneumoniaMNIST): Test AUC@0.5 (threshold fixed at 0.5).
- **Multi-class datasets**: Test MacroF1 to mitigate class imbalance effects.

We additionally report generalization gap (Train – Test) to quantify overfitting and inference time to assess suitability for edge deployment.

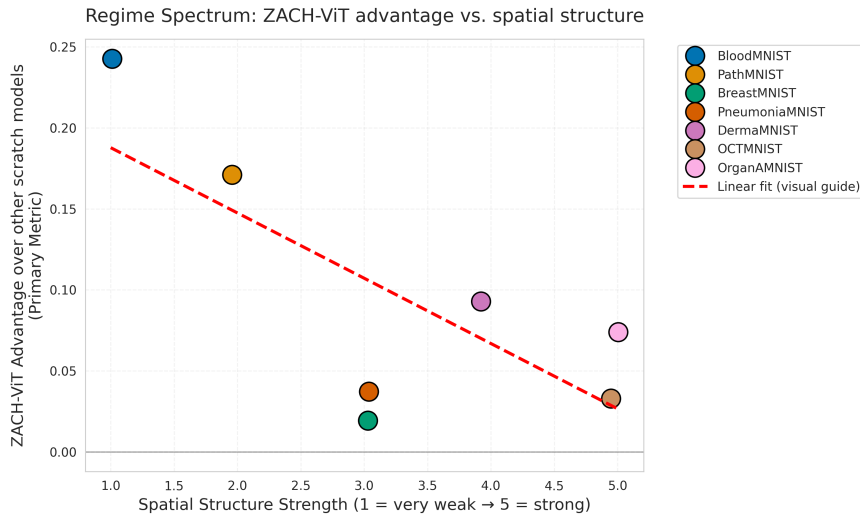


Figure 1: Regime spectrum analysis. Each point shows ZACH-ViT’s advantage over the mean performance of other scratch-trained baselines on a dataset. Datasets are ordered by an ordinal spatial-structure strength index (1 = very weak, 5 = strong). The trend suggests that ZACH-ViT’s relative advantage is larger when spatial layout is weakly informative and smaller when anatomical structure is fixed.

## 5 Results on Medical Imaging Benchmarks

Unless stated otherwise, all results in this section are reported for the full set of fifteen models summarized in Table 1.

### 5.1 Regime Spectrum Validation: When Permutation Invariance Matters

Our architectural hypothesis predicts that permutation invariance is most beneficial when spatial layout is weakly informative. Figure 1 evaluates this relationship across seven MedMNIST datasets ordered by spatial structure strength.

ZACH-ViT achieves the strongest performance among sub-1M models on BloodMNIST (MacroF1  $0.600 \pm 0.071$ ) and PathMNIST ( $0.578 \pm 0.037$ ), datasets where spatial arrangement is weakly informative. In these settings, permutation-invariant processing aligns with the data characteristics, yielding a  $+0.051$  MacroF1 gain over TransMIL on BloodMNIST, while achieving comparable (slightly lower) performance on PathMNIST ( $-0.019$  MacroF1).

Performance differences decrease on OCTMNIST and OrganAMNIST, where anatomical structure imposes strong spatial organization ( $0.247 \pm 0.052$  and  $0.436 \pm 0.036$  MacroF1). This trend supports the hypothesis: positional information contributes positively when spatial relationships are diagnostically relevant. In such cases, removing positional priors may limit modeling of fine-grained structural patterns (e.g., retinal layer organization). Overall, these results clarify the regimes in which permutation invariance is advantageous.

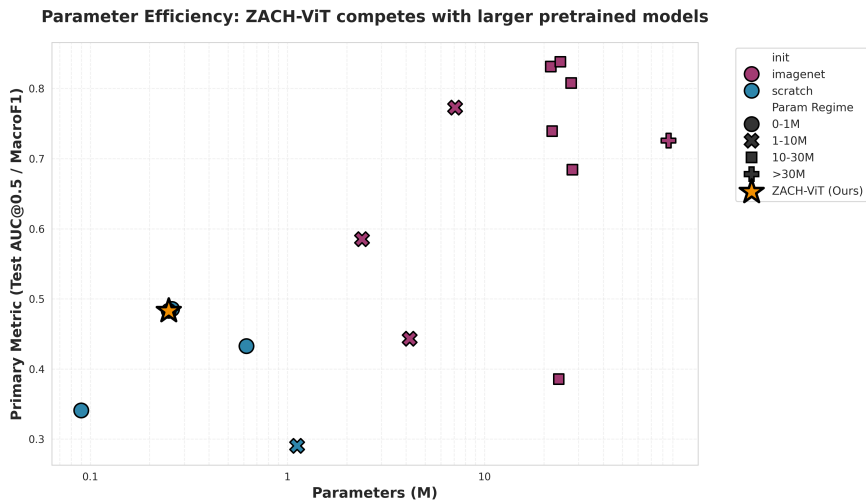


Figure 2: Global parameter efficiency across all evaluated models. ZACH-ViT competes with substantially larger pretrained architectures despite scratch training.

## 5.2 Parameter Efficiency Without Pretraining

Medical edge deployment often constrains model size and limits reliance on large pretrained networks. Figure 2 shows that ZACH-ViT achieves competitive performance with only 0.25M parameters. On BreastMNIST, performance is comparable to MobileNetV2 (2.39M parameters) despite a substantially smaller parameter budget and no pretraining. On PathMNIST, ZACH-ViT outperforms all sub-10M models except DenseNet121.

To better understand how parameter efficiency varies across spatial-structure regimes, Figure 3 provides a per-dataset decomposition. Each subplot reports model performance versus parameter count within a specific MedMNIST dataset, illustrating how the efficiency–performance trade-off changes depending on spatial structure strength. The star marker highlights ZACH-ViT. The visualization shows that ZACH-ViT remains consistently competitive among scratch-trained models across datasets, with strongest relative efficiency in weak-structure regimes (BloodMNIST, PathMNIST), while pretrained models tend to dominate regimes with stronger anatomical priors (OCTMNIST, OrganAMNIST).

This decomposition reveals that parameter efficiency is not a global property but a regime-dependent one: the same compact architecture occupies different positions on the efficiency–performance frontier depending on spatial structure strength. Consequently, evaluating edge-oriented architectures solely through aggregated performance can obscure where architectural inductive biases are most beneficial.

Importantly, although both ZACH-ViT and TransMIL exhibit permutation-invariant behavior, their architectural roles differ. TransMIL is primarily designed as a transformer-based multiple-instance learning aggregation framework operating at the bag level, whereas ZACH-ViT functions as a compact end-to-end vision backbone with direct patch-level feature learning and adaptive residual projections. This distinction helps explain why both models achieve com-

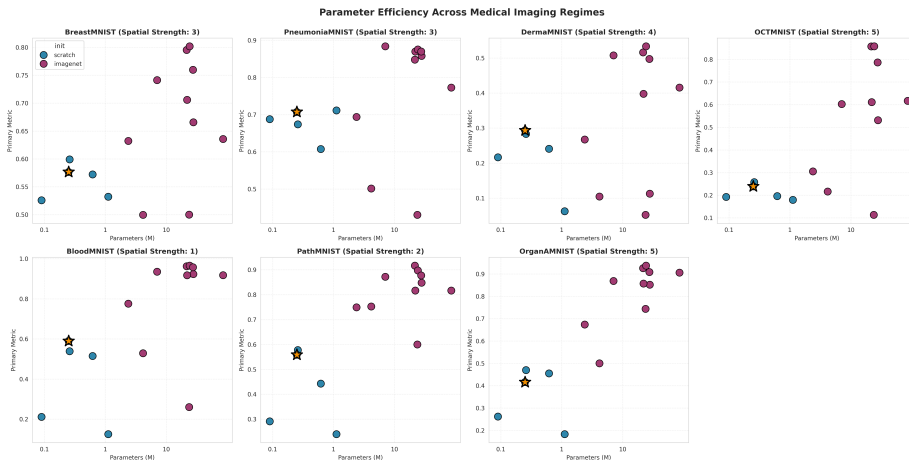


Figure 3: Parameter efficiency across individual MedMNIST datasets. Each subplot reports model performance versus parameter count within a specific spatial-structure regime. The star indicates ZACH-ViT. Results illustrate regime-dependent efficiency: ZACH-ViT shows strong competitiveness in weak-structure datasets, while pretrained models generally achieve higher performance in strongly structured anatomical regimes.

Table 2: Test MacroF1/AUC@0.5 (mean  $\pm$  std) for scratch models across MedMNIST7. Bold indicates best performer per dataset.

Dataset	Spatial Strength	ZACH-ViT	ABMIL	CNN-ABMIL	Minimal-ViT	TransMIL
BloodMNIST	1 (weakest)	<b>0.600 <math>\pm</math> 0.071</b>	0.211 $\pm$ 0.050	0.125 $\pm$ 0.067	0.515 $\pm$ 0.086	0.538 $\pm$ 0.065
PathMNIST	2	<b>0.578 <math>\pm</math> 0.041</b>	0.291 $\pm$ 0.084	0.239 $\pm$ 0.028	0.443 $\pm$ 0.061	0.577 $\pm$ 0.048
BreastMNIST	3	<b>0.577 <math>\pm</math> 0.018</b>	0.526 $\pm$ 0.058	0.532 $\pm$ 0.072	0.572 $\pm$ 0.014	0.599 $\pm$ 0.027
PneumoniaMNIST	3	<b>0.707 <math>\pm</math> 0.017</b>	0.688 $\pm$ 0.026	0.711 $\pm$ 0.042	0.607 $\pm$ 0.027	0.674 $\pm$ 0.019
DermaMNIST	4	<b>0.293 <math>\pm</math> 0.029</b>	0.216 $\pm$ 0.023	0.062 $\pm$ 0.058	0.241 $\pm$ 0.033	0.283 $\pm$ 0.024
OCTMNIST	5 (strongest)	0.239 $\pm$ 0.056	0.192 $\pm$ 0.059	0.179 $\pm$ 0.016	0.196 $\pm$ 0.069	<b>0.258 <math>\pm</math> 0.053</b>
OrganAMNIST	5	0.416 $\pm$ 0.037	0.262 $\pm$ 0.023	0.183 $\pm$ 0.055	<b>0.455 <math>\pm</math> 0.029</b>	0.470 $\pm$ 0.057

parable global ranking while exhibiting different behavior across spatial regimes and parameter-efficiency trade-offs.

This efficiency follows from removing explicit spatial encoding components and allocating capacity toward feature representation rather than positional modeling. Table 2 summarizes performance across all seven datasets, showing strong results in weak-structure regimes and competitive performance elsewhere.

### 5.3 Generalization and Edge Deployment Suitability

Robust deployment requires both generalization stability and low inference cost. Figure 4 shows that ZACH-ViT maintains small train-test gaps across datasets, indicating limited overfitting under few-shot conditions.

Figure 5 further shows that ZACH-ViT achieves low inference time relative to larger transformer models while maintaining competitive performance. Combined with its 0.25M parameter count and 2.95MB serialized footprint (Table 1), this supports deployment in resource-constrained medical environments.

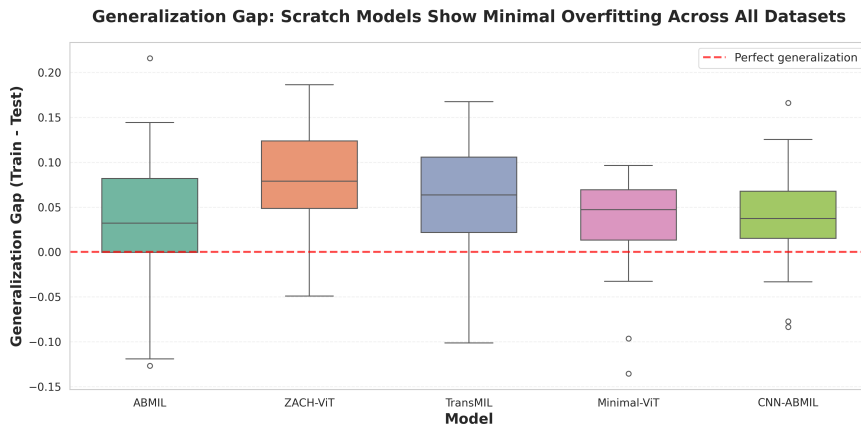


Figure 4: Generalization gap (Train–Test) for scratch models. ZACH-ViT exhibits consistently small gaps across datasets.

## 5.4 Global Ranking Analysis and Statistical Comparison

To obtain a dataset-agnostic comparison, models were ranked per dataset using AUC@0.5 (binary tasks) or MacroF1 (multi-class tasks). Mean ranks were then computed across all seven datasets.

Statistical differences were assessed using the Friedman test followed by the Nemenyi post-hoc procedure [16]. The Friedman test rejected the null hypothesis of equal performance ( $p < 0.05$ ), motivating post-hoc comparison.

Figure 6 shows mean ranks across all models. Pretrained architectures dominate aggregate ranking, with MambaOut-Tiny achieving the best mean rank (1.29), followed by DeiT-Small (2.43) and Swin-Tiny (3.14). DenseNet121 was the strongest CNN baseline (3.86). Although ZACH-ViT and TransMIL obtain identical mean ranks (10.00), indicating comparable aggregate performance across heterogeneous datasets. Despite similar aggregate ranks, the two architectures differ substantially in design philosophy: TransMIL acts as a transformer-based MIL aggregator, whereas ZACH-ViT is a compact end-to-end backbone explicitly optimized for permutation-invariant few-shot learning under strict parameter constraints.

The corresponding Critical Difference diagram (Figure 7) shows that only large rank differences reach significance due to the relatively large number of models ( $k = 15$ ) compared against seven datasets.

To isolate inductive-bias effects independent of pretraining, rankings were recomputed for scratch-trained models only (Figure 8). TransMIL and ZACH-ViT form the top group, outperforming Minimal-ViT, ABMIL, and CNN-ABMIL. The associated CD diagram (Figure 9) indicates that TransMIL and ZACH-ViT are statistically indistinguishable under this setting.

These ranking results complement the regime-spectrum analysis: pretrained models dominate aggregate rankings, whereas permutation-invariant architectures show clear advantages in weak spatial-structure regimes.

**Inference Efficiency: ZACH-ViT Achieves Competitive Accuracy with Low Latency**

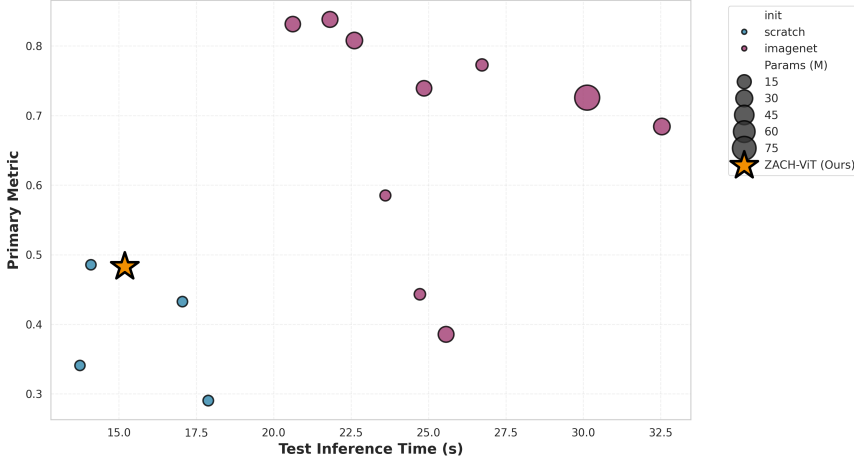


Figure 5: Inference time versus performance. ZACH-ViT occupies an efficient region of the accuracy–latency trade-off.

## 5.5 Limitations and Honest Assessment

ZACH-ViT does not universally outperform all baselines. On datasets with strong anatomical structure (e.g., OCTMNIST and OrganAMNIST), models retaining positional priors occasionally achieve higher performance. This behavior is consistent with the trade-off introduced by removing explicit spatial encoding. Overall, the results support a regime-dependent interpretation: architectural inductive bias should be matched to data structure rather than optimized for universal dominance.

## 6 Hyperparameter Sensitivity Analysis

To assess whether performance differences arise from architectural design rather than favorable hyperparameter choices, we conduct a sensitivity analysis across twelve architectural variants on BloodMNIST, representing the weakest spatial-structure regime in our spectrum. All variants follow the same training protocol (50 samples per class, five seeds {3, 5, 7, 11, 13}, batch size 16, 23 epochs), while varying only patch size, number of attention heads, transformer unit depth/width, and MLP configuration (Table 3). This setup isolates architectural effects while controlling for initialization variability.

Three observations emerge from this analysis (Figures 10–11):

**Patch size strongly influences performance.** Reducing patch size from  $16 \times 16$  to  $8 \times 8$  improves MacroF1 (+0.048 over baseline,  $p = 0.008$ ), whereas increasing patch size to  $32 \times 32$  decreases performance ( $-0.104$ ,  $p < 0.001$ ). This trend suggests that fine-grained patch decomposition better preserves discriminative local features in weak-structure data such as blood microscopy. Performance improvements are consistent across seeds (Figure 10), indicating robustness to initialization.

**Capacity scaling improves absolute performance but reduces effi-**

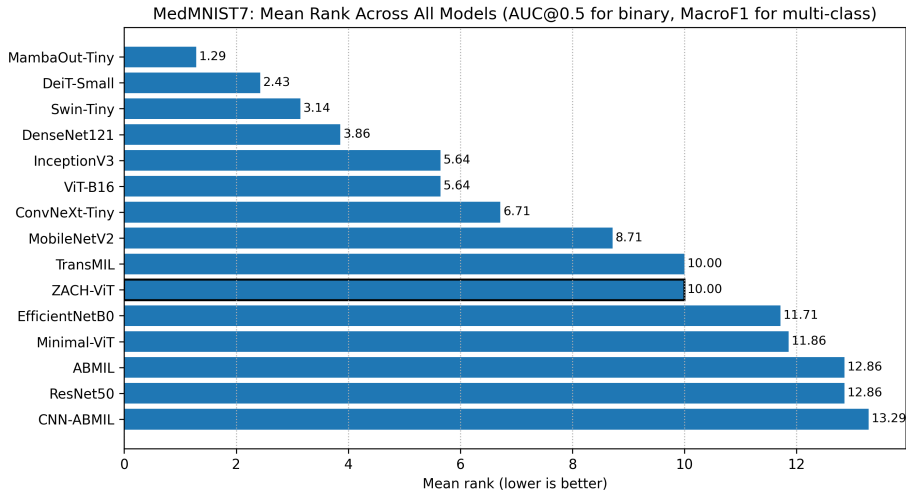


Figure 6: Mean rank across all fifteen models over seven MedMNIST datasets. Lower rank indicates better average performance.

**ciency.** The PS=8 + wider transformer unit configuration achieves the highest MacroF1 ( $0.684 \pm 0.088$ ) but requires substantially more parameters (0.60M vs. 0.25M baseline). In contrast, the PS=8 configuration with reduced parameter count (0.17M) already improves performance relative to baseline, suggesting that architectural alignment contributes more strongly than raw capacity. Figure 11 illustrates this trade-off between accuracy and parameter efficiency.

**Training remains stable across configurations.** Most variants show low variance across seeds, indicating stable optimization. Increased depth (TU=[128,128,64]) leads to higher variability without consistent performance gains, suggesting limited benefit from additional hierarchy under weak spatial structure.

Overall, this analysis indicates that performance differences are primarily associated with architectural choices—particularly patch granularity—rather than random initialization or isolated hyperparameter effects. The results further support the regime-dependent interpretation observed in the main experiments: permutation-invariant modeling benefits from configurations that preserve fine-grained local information when spatial layout is weakly informative.

## 7 Discussion

Our comprehensive validation—spanning seven medical datasets and rigorous hyperparameter sensitivity analysis—provides empirical support for the architectural hypothesis underlying ZACH-ViT. Rather than pursuing universal benchmark dominance, the results reveal a consistent relationship between architectural behavior and data structure. The regime spectrum analysis (Figure 1) shows that ZACH-ViT’s performance is systematically linked to spatial-structure strength, shifting the focus from absolute accuracy toward structural alignment with data properties and clarifying *when* and *why* the architecture succeeds. Taken together, these results suggest that architectural evaluation should explicitly account for spatial-structure heterogeneity rather than relying

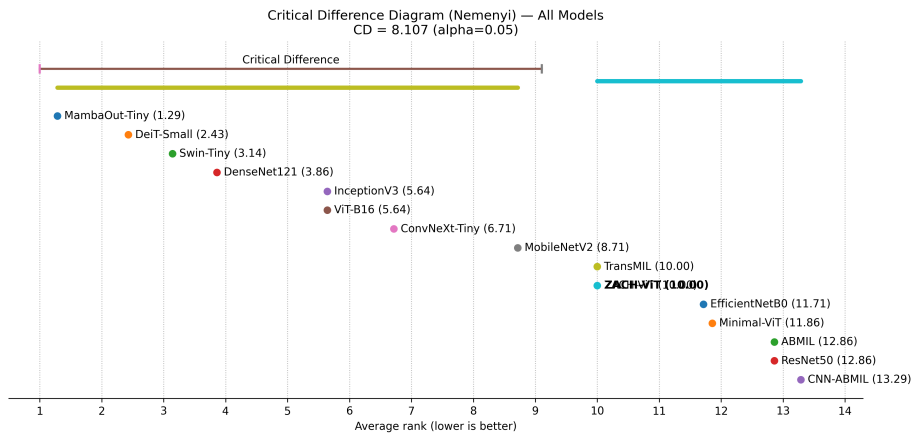


Figure 7: Critical Difference diagram (Nemenyi test,  $\alpha = 0.05$ ) for all models. Connected groups indicate non-significant differences.

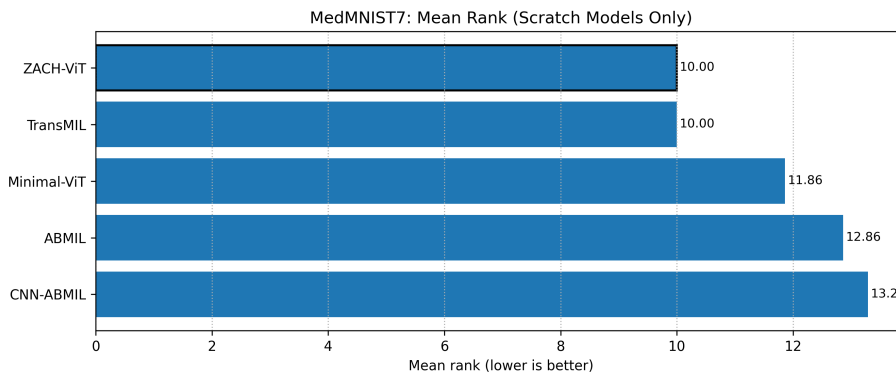


Figure 8: Mean rank restricted to scratch-trained models.

solely on aggregate benchmark performance.

**Architectural alignment outweighs scale under data scarcity.** While pretrained models generally outperform scratch-trained ones in low-data settings, ZACH-ViT closes this gap significantly within its parameter regime (0.25M vs. 2–85M). On BloodMNIST and PathMNIST—where spatial order is weakly informative—it even surpasses larger pretrained models in parameter efficiency. This suggests that for low-data regimes common in medical imaging under edge-deployment constraints, architectural parsimony aligned with data structure matters more than brute-force scaling.

**Permutation invariance enables robust generalization.** The minimal generalization gaps across all seven datasets (Figure 4) are consistent with the hypothesis that removing positional priors can reduce overfitting. Without spatial assumptions to latch onto, ZACH-ViT focuses on invariant visual features that generalize across acquisition protocols—a critical property for clinical deployment where imaging conditions vary widely.

**Edge deployment may require reconsidering architectural priors.** Most ViT variants assume spatial structure is diagnostic—an assumption that

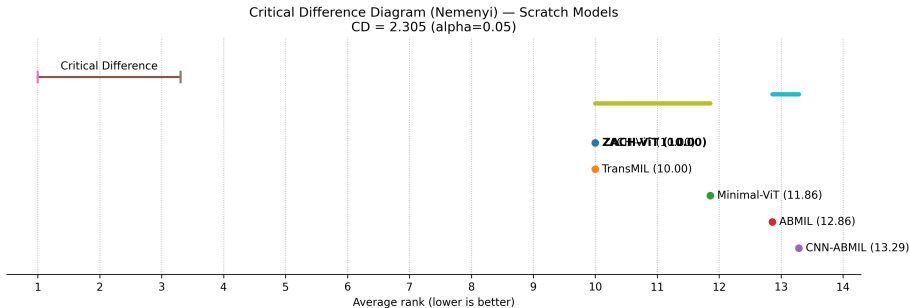


Figure 9: Critical Difference diagram (Nemenyi test,  $\alpha = 0.05$ ) for scratch-trained models.

Table 3: Hyperparameter sensitivity analysis on BloodMNIST. Test MacroF1 and accuracy are reported as mean  $\pm$  std across five seeds. Bold indicates statistically significant after correction for multiple comparisons over the baseline (two-tailed paired t-test,  $p < 0.01$ , Bonferroni correction applied across all 11 variant-vs-baseline comparisons). The baseline configuration (PS=16, H=8, TU=[128,64]) represents the primary parameter-efficient setting at 0.25M parameters. All values correspond to the final experimental protocol (23 epochs, five seeds) and replace preliminary exploratory runs used during early development.

Variant	Patch	Heads	TU	MLP	Params (M)	Test MacroF1	Test Acc	Train Time (s)	Inf Time (ms)
Baseline	16	8	128-64	128-64	0.25	0.561 $\pm$ 0.051	0.609 $\pm$ 0.054	250.1 $\pm$ 3.1	11.6 $\pm$ 0.1
<b>PS=8</b>	<b>8</b>	<b>8</b>	<b>128-64</b>	<b>128-64</b>	<b>0.17</b>	<b>0.609 <math>\pm</math> 0.038</b>	<b>0.640 <math>\pm</math> 0.035</b>	<b>310.3 <math>\pm</math> 3.6</b>	<b>13.1 <math>\pm</math> 0.2</b>
PS=32	32	8	128-64	128-64	0.54	0.457 $\pm$ 0.034	0.450 $\pm$ 0.037	252.9 $\pm$ 5.8	11.4 $\pm$ 0.2
H=4	16	4	128-64	128-64	0.25	0.579 $\pm$ 0.039	0.609 $\pm$ 0.041	253.5 $\pm$ 6.2	12.0 $\pm$ 0.5
Deeper TU	16	8	128-128-64	128-64	0.33	0.497 $\pm$ 0.095	0.516 $\pm$ 0.102	263.5 $\pm$ 1.9	12.2 $\pm$ 0.4
Wider TU	16	8	256-128	128-64	0.75	0.638 $\pm$ 0.036	0.673 $\pm$ 0.038	256.9 $\pm$ 3.8	11.5 $\pm$ 0.2
Wider MLP	16	8	128-64	256-128	0.28	0.599 $\pm$ 0.036	0.626 $\pm$ 0.038	255.4 $\pm$ 4.4	11.6 $\pm$ 0.2
PS=8 + H=4	8	4	128-64	128-64	0.17	0.599 $\pm$ 0.031	0.625 $\pm$ 0.033	281.3 $\pm$ 4.2	12.3 $\pm$ 0.3
PS=32 + H=4	32	4	128-64	128-64	0.54	0.435 $\pm$ 0.026	0.438 $\pm$ 0.028	250.8 $\pm$ 3.5	11.5 $\pm$ 0.1
Deeper+Wider	16	8	128-128-64	256-128	0.37	0.552 $\pm$ 0.036	0.575 $\pm$ 0.038	262.8 $\pm$ 2.6	11.7 $\pm$ 0.2
<b>PS=8 + Wider TU</b>	<b>8</b>	<b>8</b>	<b>256-128</b>	<b>128-64</b>	<b>0.60</b>	<b>0.684 <math>\pm</math> 0.088</b>	<b>0.713 <math>\pm</math> 0.092</b>	<b>322.0 <math>\pm</math> 3.3</b>	<b>13.7 <math>\pm</math> 0.3</b>
Wider TU + H=4	16	4	256-128	128-64	0.75	0.630 $\pm$ 0.048	0.662 $\pm$ 0.050	249.6 $\pm$ 1.4	12.4 $\pm$ 0.3

often breaks down in medical imaging scenarios where texture or local statistics dominate. ZACH-ViT’s success suggests that edge-deployed medical imaging systems benefit from architectures whose inductive biases match deployment constraints: minimal parameters, no pretraining dependency, and robustness to spatial variation. This may partially explain why many computational pathology pipelines remain confined to research environments despite strong algorithmic performance. In this sense, ZACH-ViT should be interpreted less as a lightweight alternative to existing ViTs and more as an example of architecture design driven by deployment constraints rather than benchmark conventions.

**Future directions.** While our hyperparameter sensitivity analysis supports architectural alignment as a central factor in ZACH-ViT’s performance, future work could isolate component contributions through targeted ablations (e.g., positional embeddings, pooling operators) across the spatial-structure spectrum. Such studies would provide deeper mechanistic insight into when permutation-invariant modeling is most beneficial in medical imaging.

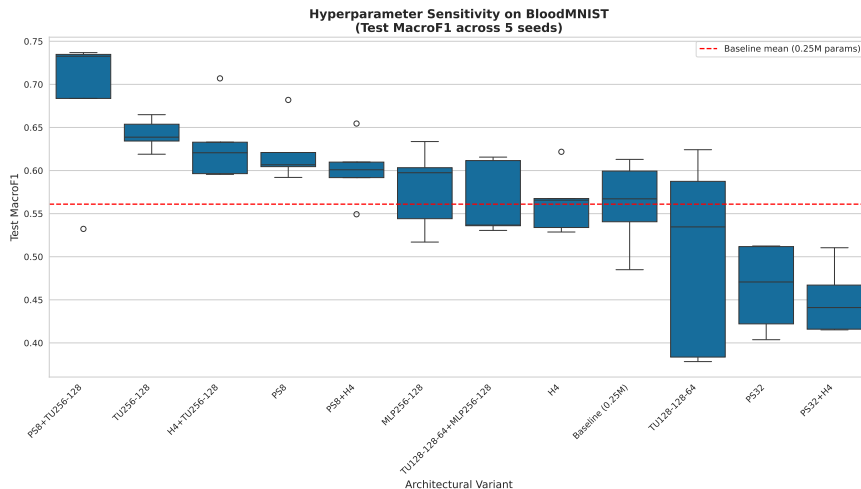


Figure 10: Hyperparameter sensitivity on BloodMNIST showing test MacroF1 distributions across five random seeds. Smaller patch sizes generally yield higher performance.

## 8 Conclusion

We introduced ZACH-ViT, a zero-token Vision Transformer that removes positional embeddings and the class token, relying instead on permutation-invariant patch processing and global pooling. Evaluation across seven representative MedMNIST datasets shows that ZACH-ViT achieves competitive performance with minimal parameters (0.25M) and no pretraining, while remaining stable under few-shot conditions where larger models often degrade. Importantly, its advantage is regime-dependent: strongest when spatial order is weakly informative (BloodMNIST, PathMNIST) and reduced when anatomical structure imposes fixed layouts (OCTMNIST, OrganAMNIST). These results support the view that architectural alignment with data structure may outweigh pursuing universal benchmark dominance.

For edge-deployed medical imaging scenarios where spatial layout is inconsistent or weakly informative, ZACH-ViT provides an alternative design strategy to conventional ViTs. Its parameter efficiency, robust generalization, and low-latency inference support deployment in resource-constrained clinical environments. More broadly, our results suggest that, under edge-deployment constraints, architectural priors should be treated as data-dependent design choices rather than default components.

## References

- [1] Dosovitskiy, A., Beyer, L., Kolesnikov, A., et al.: An Image is Worth 16x16 Words: Transformers for Image Recognition at Scale. In: International Conference on Learning Representations (ICLR) (2021)

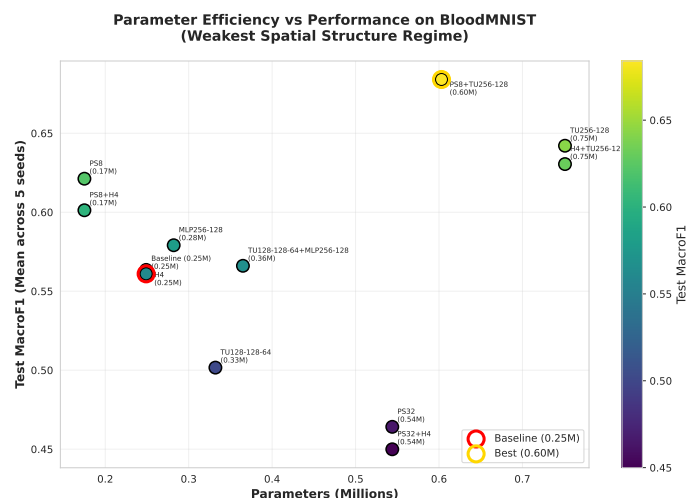


Figure 11: Parameter efficiency versus performance on BloodMNIST. Higher-performing configurations often require increased capacity, while the baseline provides a favorable efficiency–performance trade-off.

- [2] Yang, J., Huang, R., Li, J., et al.: MedMNIST v2: A Large-Scale Lightweight Benchmark for 2D and 3D Biomedical Image Classification. *Scientific Data* 10, 48 (2023)
- [3] Angelakis, A., Mousa, A., Heldeweg, M.L.A., et al.: ZACH-ViT: A Zero-Token Vision Transformer with ShuffleStrides Data Augmentation for Robust Lung Ultrasound Classification. *arXiv preprint arXiv:2510.17650* (2025)
- [4] Shao, R., Lu, M., Wang, L., et al.: TransMIL: Transformer-based Multiple Instance Learning for Whole Slide Image Classification. *Advances in Neural Information Processing Systems (NeurIPS) 34*, 21083–21096 (2021)
- [5] Gelberg, Y., Eguchi, K., Akiba, T., Cetin, E.: Extending the Context of Pretrained LLMs by Dropping Their Positional Embeddings. *arXiv preprint arXiv:2512.12167* (2025)
- [6] Ilse, M., Tomczak, J., Welling, M.: Attention-based Deep Multiple Instance Learning. In: *International Conference on Machine Learning (ICML)*, pp. 2127–2136 (2018)
- [7] He, K., Zhang, X., Ren, S., Sun, J.: Deep Residual Learning for Image Recognition. In: *IEEE Conference on Computer Vision and Pattern Recognition (CVPR)*, pp. 770–778 (2016)
- [8] Sandler, M., Howard, A., Zhu, M., Zhmoginov, A., Chen, L.C.: MobileNetV2: Inverted Residuals and Linear Bottlenecks. In: *IEEE/CVF Conference on Computer Vision and Pattern Recognition (CVPR)*, pp. 4510–4520 (2018)

- [9] Tan, M., Le, Q.V.: EfficientNet: Rethinking Model Scaling for Convolutional Neural Networks. In: International Conference on Machine Learning (ICML), pp. 6105–6114 (2019)
- [10] Huang, G., Liu, Z., Van Der Maaten, L., Weinberger, K.Q.: Densely Connected Convolutional Networks. In: IEEE Conference on Computer Vision and Pattern Recognition (CVPR), pp. 4700–4708 (2017)
- [11] Szegedy, C., Vanhoucke, V., Ioffe, S., Shlens, J., Wojna, Z.: Rethinking the Inception Architecture for Computer Vision. In: IEEE Conference on Computer Vision and Pattern Recognition (CVPR), pp. 2818–2826 (2016)
- [12] Touvron, H., Cord, M., Douze, M., et al.: Training Data-efficient Image Transformers & Distillation through Attention. In: International Conference on Machine Learning (ICML), pp. 10347–10357 (2021)
- [13] Liu, Z., Lin, Y., Cao, Y., et al.: Swin Transformer: Hierarchical Vision Transformer using Shifted Windows. In: IEEE/CVF International Conference on Computer Vision (ICCV), pp. 10012–10022 (2021)
- [14] Zhang, Z., Li, Y., Wang, Y., et al.: MambaOut: Do We Really Need Mamba for Vision? arXiv preprint arXiv:2405.15154 (2024)
- [15] Liu, Z., Mao, H., Wu, C.Y., et al.: A ConvNet for the 2020s. In: IEEE/CVF Conference on Computer Vision and Pattern Recognition (CVPR), pp. 11976–11986 (2022)
- [16] Demsar, J.: Statistical comparisons of classifiers over multiple data sets. *Journal of Machine Learning Research* 7, 1–30 (2006)